The Spectral Reflectance of Natural Surfaces

K. L. COULSON AND DAVID W. REYNOLDS
Dept. of Agricultural Engineering, University of California, Davis

(Manuscript received 21 April 1971, in revised form 28 June 1971)

ABSTRACT

The amount of solar energy reflected from various soils and types of vegetation has been measured as a function of sun elevation in six different wavelength ranges in the ultraviolet, visible and near-infrared regions of the spectrum. It is shown that there is a significant dependence of reflectance on both wavelength and elevation of the sun for all surfaces for which measurements were made.

1. Introduction

A knowledge of the reflection properties of natural surfaces for incident sunlight is required in studies of the energy balance of the earth's surface, the polarization and intensity of light from the sunlit sky, the total and spectral albedo of the earth as a planet, and in problems of remote sensing of earth resources from aircraft or satellite. Much of the previous work on surface reflection has been in determinations of reflectance of surfaces which are either illuminated from a single direction or viewed from a single direction, or both, or in measurements of the total hemispherical reflectance as determined by an inverted pyranometer or other broad-band sensor. Seldom has the hemispheric reflectance[1] been determined as a function of wavelength, and little attention has been given to the dependence of hemispheric reflectance on the direction of incidence of the radiation. The present investigation is an attempt to determine the dependence of hemispheric reflectance of various natural and selected man-made surfaces on both spectral distribution and direction from which the light is incident on the surface.

Perhaps the most extensive series of observations of the spectral reflectance of natural surfaces is that of Krinov (1947), in which measurements made on several types of natural surfaces show total reflectance values of soil and rocks varying from as little as 0.02 for black sandy loam to as much as 0.35–0.75 for highly reflecting clay, limestone and shale. Although Krinov's measurements were taken mainly in a small solid angle oriented in either the nadir direction or at a 45° nadir angle at an azimuth of 90° from that of the sun, the data show the general wavelength dependence of reflectance in the visible and near-infrared spectral regions. Gates *et al.* (1965) determined the spectral reflection properties of plants when viewed in the direction of the surface-normal, while Coulson *et al.* (1965a,b) obtained similar measurements for several types of surfaces as a function of viewing angle for a given angle of incidence. Ashburn and Weldon (1956) measured the diffuse reflectance of desert surfaces as a function of sun elevation and observed a dependence of reflectance on sun elevation similar to that obtained in the present series. The extensive work done on surface reflectance recently in the Soviet Union, particularly with respect to water surfaces, is summarized by Kondratyev (1969) and the problem is discussed in more detail by Mullaama (1964). The reflectance of particular types of surfaces, especially those with complex structure, has been extensively studied in connection with the lunar and planetary programs (Hapke and Van Horn, 1963; Salisbury and Glaser, 1964; Oetking, 1966; Orlova, 1952; and others). Many of the available measurements have been tabulated and summarized by Earing and Smith (1966). Attempts to describe surface reflectance by theoretical methods have been made by Shifrin (1953), Hapke (1963), Ross and Nil'son (1963, 1968), and Barkas (1939), among others.

[1] The term hemispheric reflectance is chosen as being more specific than the generally equivalent terms of surface albedo or directional reflectance. Hemispheric reflectance is used here as the ratio of the energy reflected into the outward hemisphere to that incident on the (horizontal) surface, and is applied to relatively narrow spectral regions. The term albedo is often loosely applied, but it is usually taken as the ratio of reflected to incident energy integrated over the entire solar spectrum. The term directional reflectance conjures up the concept of the ratio of energy reflected in a given direction to that incident on the surface, which is not the quantity discussed here.

2. Instrumentation and procedures

The present series of measurements were made with a filter type radiometer fitted with an integrating sphere as the primary radiation receiver. A schematic diagram of the instrumentation is shown in Fig. 1. Measurements were made in six spectral ranges from the ultraviolet to the near-infrared, the specific wavelengths being defined

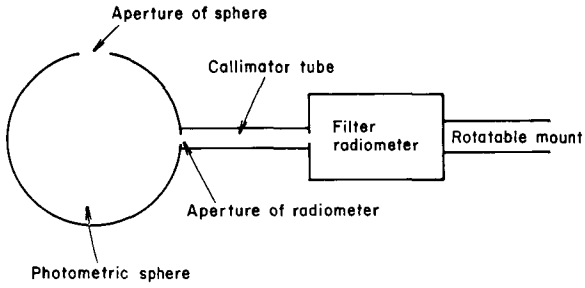

FIG. 1. Schematic diagram of filter radiometer fitted with an 8-inch diameter photometric sphere and mounted in such manner as to permit 180° rotation around a horizontal axis.

by narrow band (~100 Å half-width) interference filters. The effective wavelength sensitivity of the instrument, represented by the product of filter transmissivity and relative sensitivity of the S-20 photomultiplier tube, in the six spectral regions is shown in Fig. 2. In operation, a single determination of the hemispheric reflectance of a surface required three separate measurements of the radiant flux into the aperture of the integrating sphere, the aperture being a 1.5-inch diameter hole in the wall of the sphere at an angle of 90° from the entrance aperture of the radiometer itself. The first measurement was of the total downward flux $F_\lambda\downarrow$ across a horizontal surface and confined to the wavelength interval of the interference filter, the horizontal surface being the plane of the aperture of the integrating sphere and of area equal to that of the aperture. Obviously $F_\lambda\downarrow = F_{D\lambda} + F_{d\lambda}$, where $F_{D\lambda}$ is the component due to the direct solar beam and $F_{d\lambda}$ is that due to the diffuse skylight. The second measurement was of the diffuse component $F_{d\lambda}$ only, the measurement being obtained by shading the aperture from the direct solar beam by use of a small opaque disk. Then by taking the difference $F_\lambda\downarrow - F_{d\lambda}$, we obtain the direct flux $F_{D\lambda}$, which is used later in computing a correction for the shadow of the instrument. The third quantity measured was the total upward flux $F_\lambda\uparrow$ of radiation reflected from the surface, the measurement being obtained by simply rotating the sphere around a horizontal axis so that the aperture opened downward instead of upward. Then the hemispheric reflectance A_λ (albedo) of the surface at wavelength λ is given by the ratio

$$A_\lambda = F_\lambda\uparrow / F_\lambda\downarrow. \quad (1)$$

Since the total set of three measurements could be made in less than 2 min, changes of the incident radiation during the period were neglected. There is some evidence, however, that this neglect was responsible for an appreciable amount of scatter in the data points on days with considerable haze. The radiometer signals were recorded in most of the measurements on digital magnetic tape, and all data reduction was by computer methods. Thus, human errors in the data were kept at a minimum.

The one correction that was systematically applied to the data was to compensate for shading of the surface by the instrument itself. For this correction we assumed that the surface shading applies only for the direct radiation, since this is generally the dominant component, and some compensation for surface shading by the instrument is contributed by reflection of both direct and diffuse components from instrument to sur-

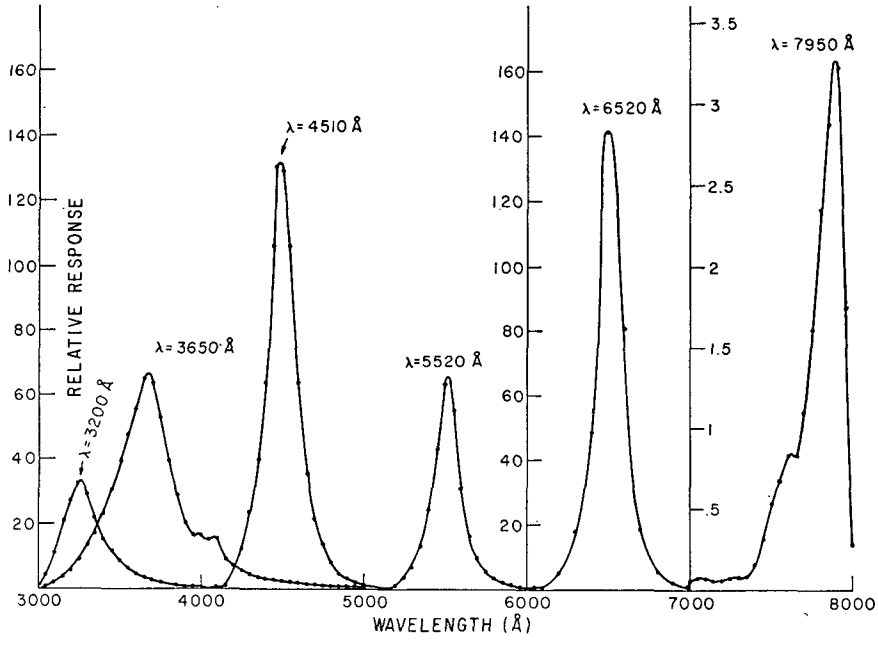

FIG. 2. Relative response to solar radiation of the reflectometer system containing six optical interference filters in combination with the S-20 photocathode of the photomultiplier tube.

face. The solid angle ω of the surface shadow subtended at the entrance aperture is

$$\omega=\frac{a\cos^3\theta_0}{h^2}, \tag{2}$$

where a is the area of the shadow in units of aperture area, h the height of the aperture above the surface, and θ_0 the zenith angle of the sun. The increment $\Delta F_\lambda\uparrow$ which would have been contributed to the measured flux $F_{m\lambda}\uparrow$ in the absence of shadow is

$$\Delta F_\lambda\uparrow=\frac{\omega}{2\pi}AF_{D\lambda}\cos\theta_0, \tag{3}$$

where the reflected energy is assumed isotropic in the outward hemisphere. This is a reasonable assumption, since the shadow subtends a relatively small solid angle and any non-isotropic intensity distribution would introduce only second-order effects which can be neglected. Obviously,

$$F_\lambda\uparrow=\Delta F_\lambda\uparrow+F_{m\lambda}\uparrow. \tag{4}$$

Since $\Delta F_\lambda\uparrow\ll F_{m\lambda}\uparrow$, we are justified in replacing A_λ in Eq. (3) by an approximate reflectance A_λ', where

$$A_\lambda'=F_{m\lambda}\uparrow/F_\lambda\downarrow, \tag{5}$$

in order to avoid iteration in computing A_λ. It is interesting to see, by combining Eqs. (2) and (3), that $\Delta F_\lambda\uparrow$ is a strong function of θ_0, being proportional to $\cos^4\theta_0$.

3. Results of measurements

The results to be discussed consist of a set of measurements of hemispheric reflectance in six wavelength ranges taken at a rate of about one data point every 2 min from before sunrise to solar noon for each of eleven types of surfaces. The measurements have been taken at Davis, Calif., over a three-year period, the schedule being adjusted to emphasize the time around the summer solstice in order to extend the measurements to the highest sun elevations possible. The data are shown in several plots of hemispheric reflectance vs sun elevation, and the plots are arranged by surface type, with mineral surfaces first.

a. Hemispheric reflectance of mineral surfaces

1) YOLO LOAM SOIL, DRY, DISKED

This soil gets its designation from Yolo County, Calif., and consists of a combination of clay (particle diameters $d<2\,\mu$), silt ($2\,\mu\leqslant d\leqslant 50\,\mu$), and sand ($50\,\mu<d<2$ mm). The surface texture for these measurements was mainly of small clods of soil ranging in size from a few millimeters up to 10 cm in diameter, with the interstices filled with finer material. The surface had recently been disked, resulting in disk marks (small ridges and valleys of a few centimeters amplitude) oriented in a north-south direction.

Curves of hemispheric reflectance vs sun elevation for this dry Yolo loam soil are shown for six different wavelengths in Fig. 3. The increase of reflectance with increasing wavelength is a general characteristic of mineral surfaces for wavelength ranges in the visible and in the near-infrared out to the water absorption bands beyond $\lambda=1\,\mu$. In the ultraviolet, however, the wavelength dependence of reflectance is relatively small, as shown in the diagram.

The maximum of hemispheric reflectance A_λ vs sun elevation h shown by the curves for $h\leqslant 10°$ is qualitatively similar to that first observed by Ashburn and Weldon (1956) for a desert surface. However, the maximum is by no means as pronounced for this soil surface as they found for the desert, and the maximum here occurs at lower sun elevations than that for the desert surface. For instance, at $\lambda=0.55\,\mu$, the desert maximum occurred at $h\approx 12°$ with a value 14% higher than that at $h=60°$.

The variation of hemispheric reflectance with wavelength is shown explicitly in the plot of A_λ vs λ in Fig. 4. Of particular interest is the increase of A_λ with a decrease of λ from $\lambda=0.365\,\mu$ to $0.320\,\mu$ at the lower sun elevations. This effect was not seen for other surfaces studied, and it needs further verification.

2) YOLO LOAM SOIL, WET, PUDDLED

The soil surface for this set of measurements was sprinkled for several hours during the afternoon and night before measurements were started at daybreak. The surface was completely wet and remained so throughout the measurement period, but there was no

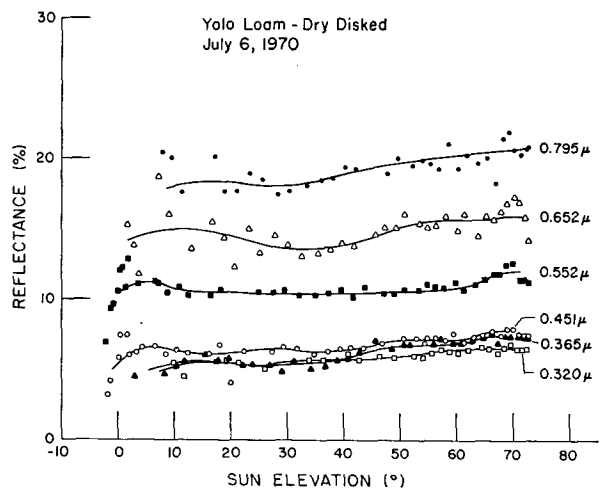

FIG. 3. Hemispheric reflectance of dry Yolo loam soil at six different wavelengths, as a function of elevation of the sun. The surface was marked by small ridges and valleys produced by tilling with a disk.

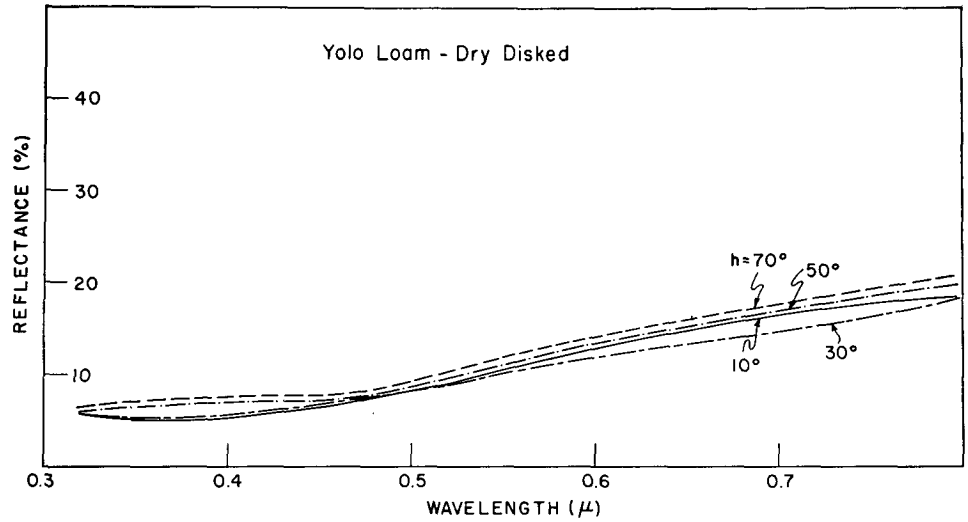

FIG. 4. Hemispheric reflectance of dry Yolo loam soil as a function of wavelength for four different elevations of the sun.

standing water on the surface. The sprinkling process had broken up the larger soil agglomerates and erased any tillage marks in the soil, resulting in a very flat and essentially featureless wet soil surface for the measurements.

The variation of hemispheric reflectance A_λ with sun elevation h is shown for six wavelengths in Fig. 5. There appears to be a small but definite decrease of A_λ with increasing h for $h>20°$, although the decrease is embedded in considerable variation in the data points themselves. At lower sun elevations the increase of A_λ with increasing h is present but not pronounced.

The increase of A_λ with increasing λ is much less pronounced here than for the previous case, particularly at $\lambda>0.652\,\mu$. The physical reason for this effect is no doubt the well-known decrease of reflectance of water with increasing wavelength tending to offset the reflectance properties of the soil particles themselves.

3) YOLO LOAM, DRY, PUDDLED

This was the same surface as that of the previous section, except that the soil was permitted to dry out for eight days before the measurements were repeated. The configuration of the surface appeared to be un-

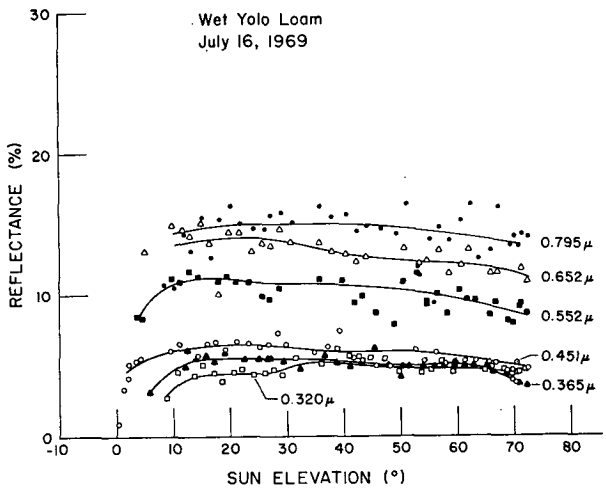

FIG. 5. Hemispheric reflectance of wet Yolo loam soil at five different wavelengths, as a function of elevation of the sun. Sprinkling for several hours had erased most of the details of the soil surface.

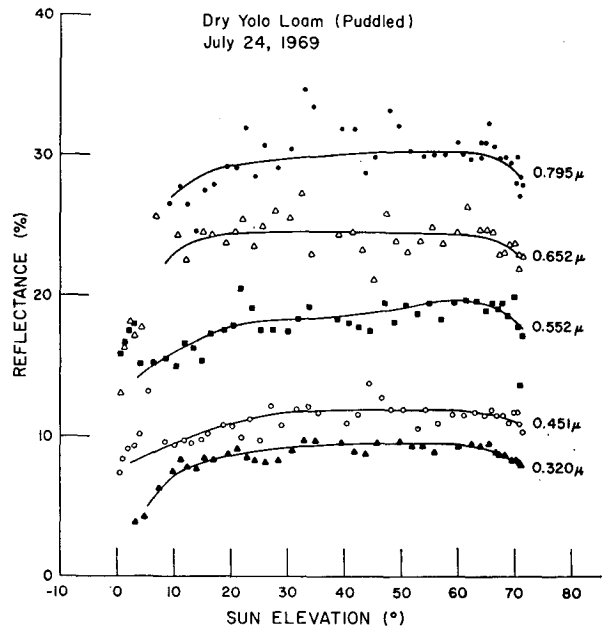

FIG. 6. Hemispheric reflectance of dry Yolo loam soil at five different wavelengths, as a function of elevation of the sun. This was the same surface as that for the data of Fig. 5 except that it had been allowed to become completely dry for these measurements.

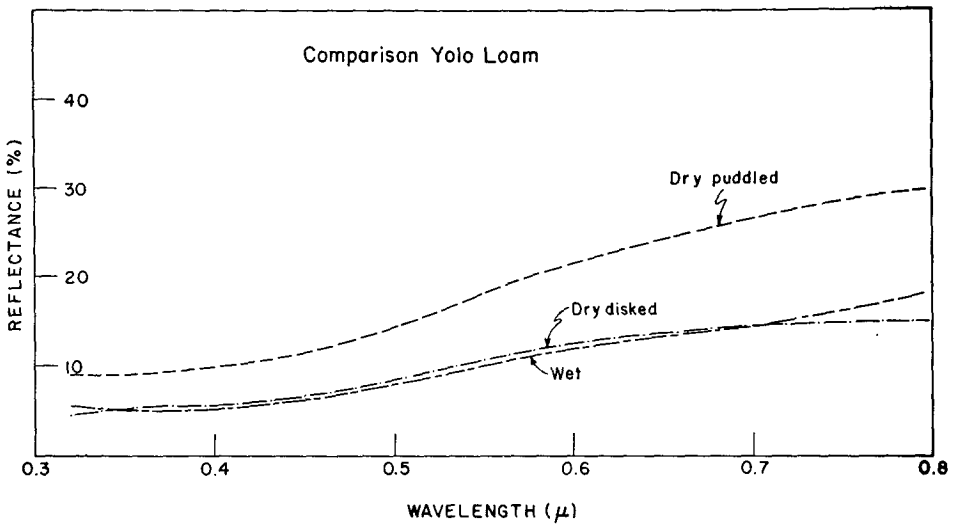

FIG. 7. Hemispheric reflectance of Yolo loam soil for three different surface conditions, as a function of wavelength. The data are for a sun elevation of 30°.

changed during the drying process. The results of the measurements are shown in Fig. 6. The general configuration of the curves is not greatly different from those of the disked soil (Section 1). However, the reflectance for this smoothed surface is about 50% higher than that of the disked surface, both being in the dry state. Drying of the previously wet surface increased its reflectance by a factor of ~ 2 at all wavelengths as can be seen by comparing Fig. 5 with Fig. 6.

The relatively pronounced downward slope of the curves in Fig. 6 at $h > 60°$ appears to be well defined by the data points, but it is much less evident for other surfaces and it probably needs verification by additional measurements.

A comparison of the reflectance for the three different types of Yolo loam surface (disked and dry, puddled and wet, and puddled and dry) is shown in Fig. 7 for a sun elevation of 30°. The large agglomerates, with their attendant shadows, rendered the disked surface reflectance only slightly higher than that of the wet surface, whereas the smaller agglomerates and individual particles of the puddled soil resulted in a greatly enhanced reflectance at all wavelengths for which measurements were made.

4) SACRAMENTO CLAY

Sacramento clay is an extremely heavy clay and silt soil occurring in the Sacramento River valley in California. The small particle sizes make the soil relatively impervious to water, a fact which accounts for the main agricultural use for the soil being that of growing rice. In its dry state the soil has a medium gray color. When the soil is tilled it breaks up into agglomerates of a few millimeters to several centimeters in size, and there is no finer material filling in the interstices of the coarse granular texture.

The hemispheric reflectance of this clay is shown as a function of sun elevation for five different wavelengths in Fig. 8. The curve for $\lambda = 0.365\,\mu$ is not shown, as it is almost identical to that for $\lambda = 0.320\,\mu$. The most obvious characteristic of the curves is a strong decrease of reflectance with increasing sun elevation for $h > 10°$. The physical reason for the effect is not completely known, but it is probably due to the complex of open spaces among the coarse particles. Radiation which enters the spaces is largely trapped within the structure, and, of course, the fraction of incident radiation entering the spaces increases with increasing sun elevation.

The wavelength dependence of reflectance for the Sacramento clay is very similar to that shown above for Yolo loam soil, the reflectance at $\lambda = 0.80\,\mu$ being approximately twice that at $\lambda = 0.32\,\mu$.

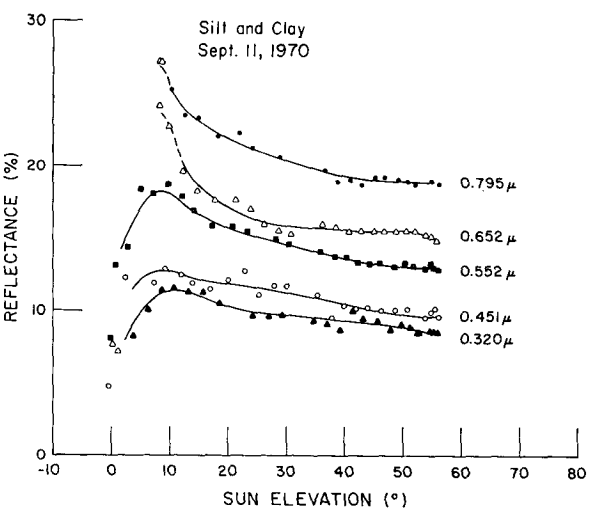

FIG. 8. Hemispheric reflectance of Sacramento clay soil at five different wavelengths, as a function of sun elevation.

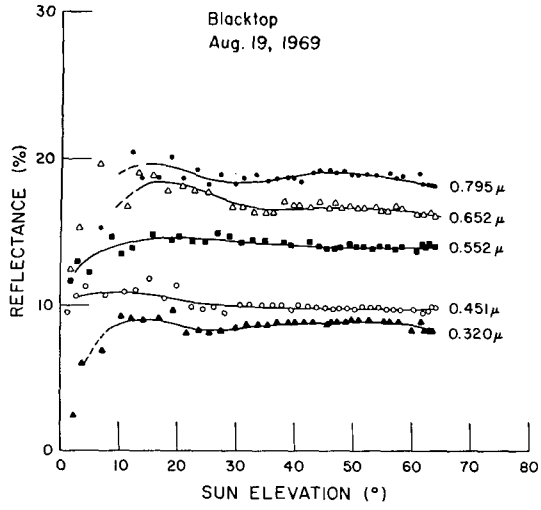

FIG. 9. Hemispheric reflectance of blacktop at five different wavelengths, as a function of sun elevation.

5) BLACKTOP (ASPHALT, MACADAM)

This blacktop surface is that of a parking lot in Davis. Aside from the fact that it has a low traffic load and is therefore essentially uncontaminated by oil or other traffic film, the surface is similar to that of many blacktop roads and highways. The parking lot is several years old, relatively light colored, and has a generally smooth texture. Exposed pebbles of naturally smooth gravel are visible over approximately 75% of the surface area.

The low reflectance which would be expected for blacktop is seen in the curves of reflectance A vs sun elevation h in Fig. 9, and A is to a first approximation independent of h. This latter feature is probably due to the virtual lack of shadows on the relatively smooth surface of the blacktop. The increase of reflectance with increasing wavelength typical of mineral surfaces is shown by the curves of A vs λ in Fig. 10.

b. Hemispheric reflectance of green vegetation

The reflection properties of green plants are of interest to agriculturalists, plant physiologists, ecologists, and scientists interested in remote sensing of the environment. Measurements of spectral reflectance of plants are numerous and well documented (e.g., Krinov, 1947; Gates and Tautraporn, 1952).

Although there are large differences among different types of plants, a typical reflectance spectrum of green vegetation shows low values in the ultraviolet and blue regions ($\lambda<0.48\,\mu$), slightly larger values in the green ($\lambda\approx0.54\,\mu$), low values again in the red ($\lambda\approx0.65\,\mu$), and a very strong increase for $\lambda>0.70\,\mu$ leading to high values in the regions 0.8–1.3 μ, 1.6–1.8 μ, and 2.1–2.3 μ. Plant pigments, particularly chlorophyll, have strong absorption bands in the blue ($\lambda\approx0.45\,\mu$) and red ($\lambda\approx0.65\,\mu$) regions, and liquid water has several strong absorption bands in the near-infrared at $\lambda>0.9\,\mu$. Because these features are already well documented, they will not be discussed at length here. However, selected wavelength distributions which are typical of green vegetation will be shown with the spectral characteristics being implicit in all of the reflectance data.

The surfaces for these measurements of hemispheric reflectance of plants have been chosen to represent several different leaf types and stages of plant development. Alfalfa and sugar beets represent broad-leaf plants with small and large leaves, respectively. The leaves for these plants have a generally quasi-horizontal orientation. Bluegrass and immature rice plants, on the other hand, have thin leaves with a mainly vertical

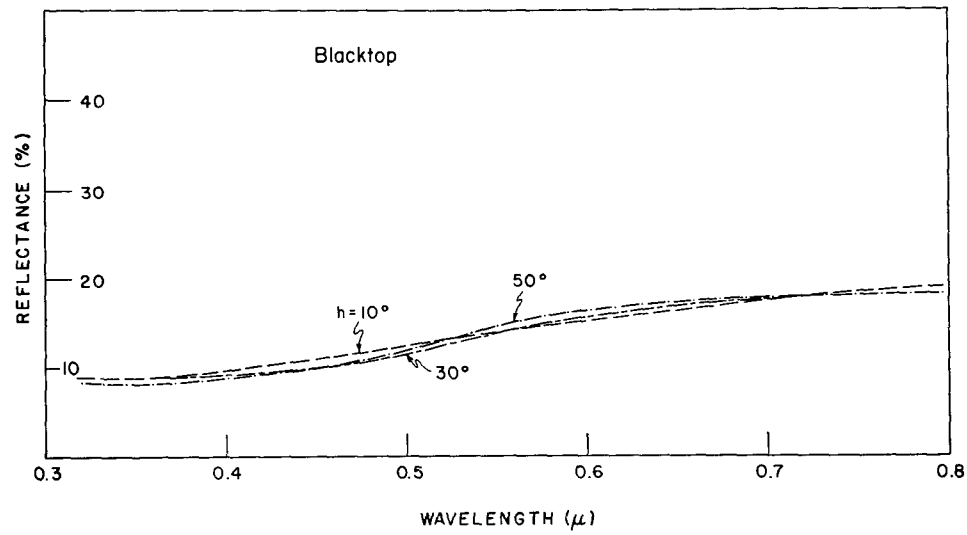

FIG. 10. Hemispheric reflectance of blacktop as a function of wavelength for three different elevations of the sun.

orientation. Rice plants after head emergence and sorghum (milo) in the fully mature stage represent a complex of surfaces with all orientations, and a combination of leaf and grain surfaces. Reflectance data for each of these types are shown below.

1) ALFALFA

The hemispheric reflectance of a thick stand of growing alfalfa, ~1 ft high, is shown as a function of sun elevation in Fig. 11. The obvious features of the diagram is the very high reflectance at $\lambda=0.79\,\mu$ and the general decrease of reflectance with increasing sun elevation. This latter feature is probably a result of the radiation being increasingly trapped within the interstices of the complex surface as the relative amount which enters the surface increases as the incident direction approaches the surface normal. The reflection maximum at $h\approx 10°$, first observed by Ashburn and Weldon (1956) for a desert surface, is clearly evident in the diagram.

The dependence of reflectance on wavelength shown by the curves of Fig. 12 is typical of green plants in general. Plant pigments reflect ultraviolet, blue and red wavelengths weakly, whereas there is a secondary maximum of reflectance in the green region. This fact, together with the spectral distribution of sunlight and of eye sensitivity, is responsible for the green color of this stand of alfalfa and most other growing plants. The near-infrared wavelengths, however, are absorbed very little by most plant pigments. Thus, infrared radiation

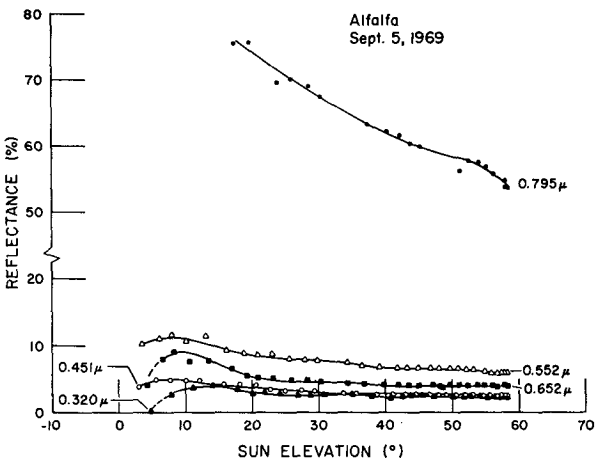

FIG. 11. Hemispheric reflectance of growing alfalfa at five different wavelengths, as a function of sun elevation. (The scale for this and later diagrams has a discontinuity between the curves for $\lambda=0.552\,\mu$ and $\lambda=0.795\,\mu$.)

is allowed to enter the main cellular structure of the plant tissues, where large differences of refractive index between the cells and cell walls are effective in producing a large reflectance of the plant at infrared wavelengths.

2) SUGAR BEETS

The sugar beet plant, the above-ground structure of which consists mainly of large leaves of quasi-horizontal

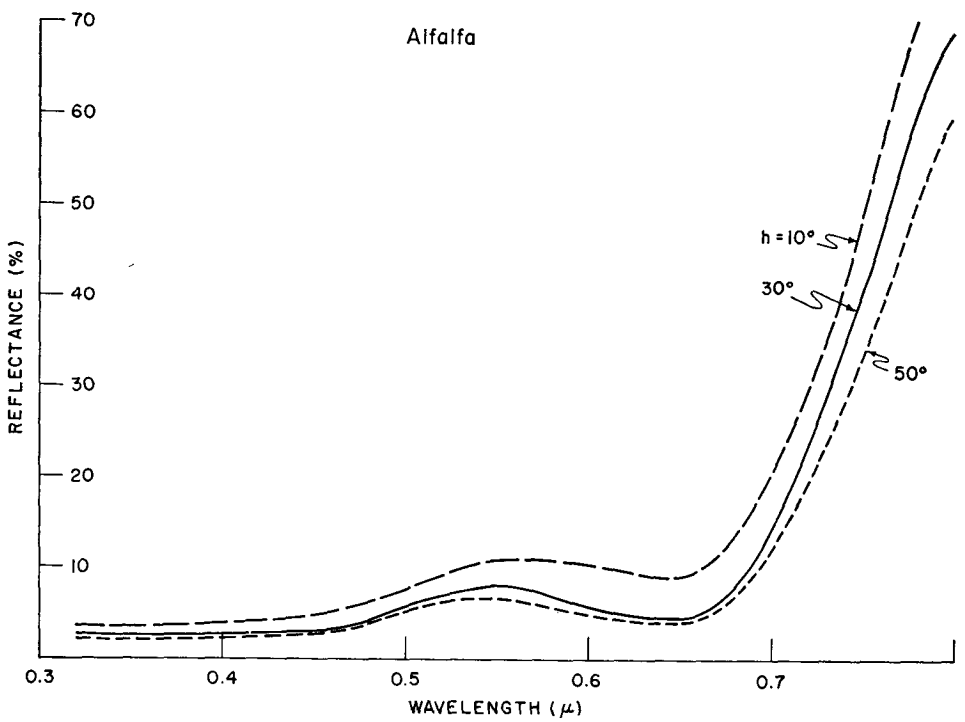

FIG. 12. Hemispheric reflectance of growing alfalfa as a function of wavelength for three different elevations of the sun.

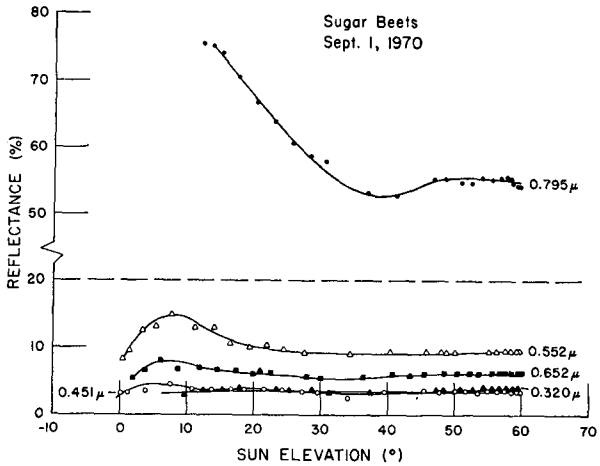

FIG. 13. Hemispheric reflectance of growing sugar beets at five different wavelengths, as a function of sun elevation.

orientation, does not present as many interstices within the canopy as does alfalfa and many other plants. Thus, one would not expect as much change of reflectance with such complex plant surfaces. This expectation is borne out by the curves of Fig. 13, in which reflectance in the visible and ultraviolet wavelengths is almost independent of sun elevation for $h>10°$. The somewhat complicated configuration of the curve for $\lambda=0.795\,\mu$ is difficult to explain, but it does appear to be well substantiated by the measurements.

3) BLUEGRASS TURF

Curves of hemispheric reflectance vs sun elevation for a well-kept bluegrass lawn are shown in Fig. 14. As with most bluegrass turf, the grass blades were almost all standing upright, thereby creating a relatively uniform surface with many interstices. The grass had been recently mowed to a height of ~2 inches.

There are two main differences between the reflectances curves for bluegrass and those for the broad-leafed sugar beets, shown by Figs. 14 and 13, respectively. First, the reflectance of sugar beets is somewhat higher at $\lambda=0.795\,\mu$ than is that for bluegrass. The fact that the effect is most pronounced at the higher sun elevation indicates a trapping of the radiation within the interstices of the bluegrass. Secondly, the general decrease of reflectance at all wavelengths with increasing sun elevation for bluegrass but not for sugar beets also indicates more radiation trapping by bluegrass than by sugar beets.

4) RICE, IMMATURE STAGE

The highest infrared reflectance of any of the surfaces studied was exhibited by rice plants before emergence of the heads of grain, as shown by Fig. 15. The rice crop for these measurements was standing in water, but the plants were thick enough so that no water surface was visible from above the 3-ft high plants. The reason for the particularly high infrared reflectance of this crop has not been determined. As in previous cases, trapping of radiation by the interstices of the complex surface is probably responsible for the decrease of reflectance with increasing sun elevation.

5) RICE, AFTER HEAD EMERGENCE

The reflectance of rice plants was significantly increased in the visible and ultraviolet regions by the emergence of the grain-bearing heads, as shown by the

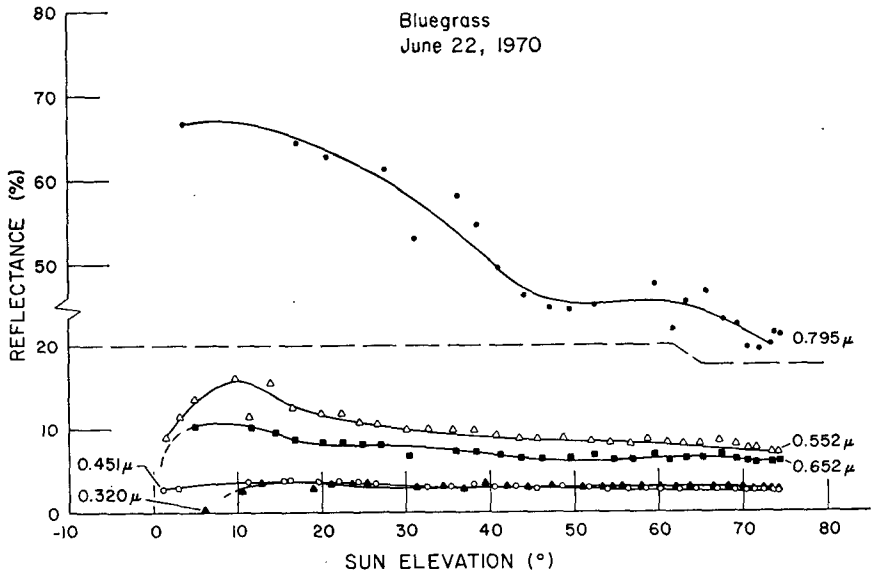

FIG. 14. Hemispheric reflectance of green bluegrass turf at five different wavelengths, as a function of sun elevation.

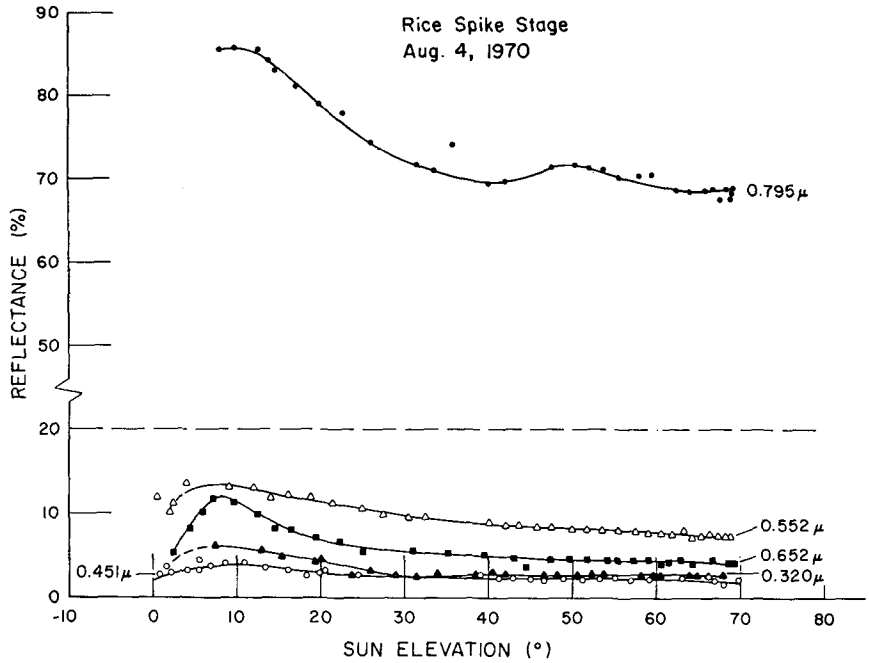

FIG. 15. Hemispheric reflectance of a field of growing rice at five different wavelengths, as a function of sun elevation. These data were taken before the emergence of the grain-producing heads.

curves of Fig. 16. This would be expected, as the still unripe heads appear considerably lighter than the dark green background of foliage. A significant fraction of infrared wavelengths, however, must be absorbed by the rice grains, as the data show a decrease of reflectance of 10% or more on emergence of the heads.

6) SORGHUM (MILO), MATURE STAGE

The crop of sorghum for which the reflectance measurements of Fig. 16 were taken was ~4 ft high and fully mature. The heads, well developed and ripe, were principally of reddish color, but at least 90% of the foliage was still green. While the individual plants were large and full, they were widely enough spaced so that the Yolo loam soil was visible over perhaps half of the area when viewed directly downward from above the plants.

As can be seen from the data of Fig. 17, the infrared reflectance of this composite grain-foliage-soil surface was generally much lower than that of green foliage alone, whereas the reflectance in the ultraviolet, blue,

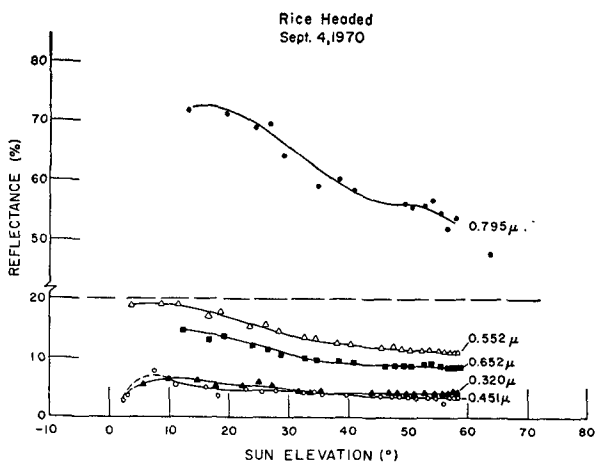

FIG. 16. Hemispheric reflectance of a field of rice after emergence of the grain-bearing heads. The data are for five different wavelengths and plotted as a function of sun elevation.

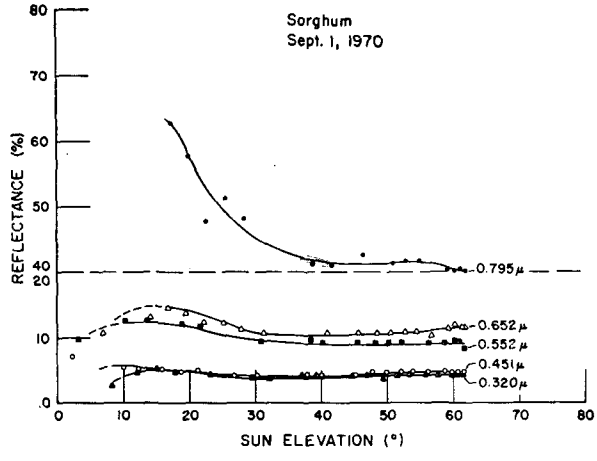

FIG. 17. Hemispheric reflectance of a field of mature sorghum (milo) at five different wavelengths, as a function of sun elevation. The reflecting surface was a complicated combination of heads of grain, green leaves, and the underlying soil.

green, and particularly the red wavelengths was higher than that of green foliage. No doubt, both the grain and the dry soil contributed to the increase of reflectance in these spectral regions. The marked decrease of infrared reflectance with increasing sun elevation for $h<35°$ is probably due to a relative increase of radiation reaching the surface and being absorbed by the soil as the rays of the sun become more normally oriented and thereby penetrate the plant canopy more efficiently.

4. Summary and conclusions

These measurements of the hemispheric reflectance of natural surfaces exhibit the following characteristics and appear to substantiate the following conclusions:

1) The reflectance of mineral surfaces, including various types of soils and blacktop, generally increases with increasing wavelength throughout the wavelength region $\lambda=0.320$–$0.795\,\mu$.

2) The reflectance of green vegetation shows a typical pattern of very low values in the ultraviolet, blue and red spectral regions, a secondary maximum in the green region, and a very strong increase to high values in the near-infrared region of the spectrum. Low values occur in regions of strong absorption by plant pigments, whereas penetration of plant tissue and a large amount of reflection at cell walls is the main process responsible for high values of reflectance in the infrared.

3) The reflectance of most surfaces appears to reach a maximum at sun elevations of 10–20°. This apparent reflection maximum, while not completely understood, is probably the result of a combination of two effects. First, observations show that most surfaces have a higher reflectance for light incident at a large zenith angle than for that at more nearly normal incidence. This would explain the decrease of reflectance with increasing sun elevation for the portion of the curve subsequent to the maximum. Second, the ratio of direct to diffuse light undergoes a rapid shift at low sun elevations. Obviously, the incident light is entirely diffuse when the sun is below the horizon, and since the major part of the diffuse flux is from zenith angles which are not large, the reflectance of the surface is relatively low at that time. This is shown by the curves. As the sun increases in elevation the relative contribution of diffuse light decreases with respect to direct light, and since the direct light is incident at a large angle, it is more strongly reflected than is the diffuse light. This explains the increasing reflectance observed at low sun elevations. Finally, the two opposing effects will just balance each other, thereby producing no change of reflectance, at some elevation of the sun. This point of maximum reflectance is seen by the curves to occur at a sun elevation of 10–20°.

4) Surfaces of a complex nature which contain many interstices within the structure generally show a decrease of reflectance with increasing sun elevation. It is probable that this feature is caused by a significant part of the incident radiation being trapped within the interstices, in a manner similar to that in other types of optical traps.

5) Additional measurements of this type for other natural surfaces would be useful in many types of investigations, including studies of the atmospheric and surface energy budgets and remote sensing of the environment. They are particularly useful in studies of the polarization and intensity of light directed either outward to space from the earth or downward toward the surface from the sunlit sky. This latter feature was the motivation for initiating the present series of measurements.

Acknowledgment. We would like to thank Messrs. Timothy Cummings and Bruce Jackson for their assistance in the field work and data reduction, and to express our appreciation for support of the research to the Air Pollution Control Office (Grants 00742 and 00743) and to the National Aeronáutics and Space Administration (Grant NGL-05-003-404).

REFERENCES

Ashburn, E. V., and R. G. Weldon, 1956: Spectral diffuse reflectance of desert surfaces. *J. Opt. Soc. Amer.*, **8**, 583–586.

Barkas, W. W., *1939*: Analysis of light scattered from a surface of low gloss into its specular and diffuse components. *Proc. Phys. Soc. (London)*, **51**, 274–295.

Coulson, K. L., G. M. Bouricius and E. L. Gray, 1965a: Optical reflection properties of natural surfaces. *J. Geophys. Res.*, **70**, 4601–4611.

——, E. L. Gray and G. M. Bouricius, 1965b: A study of the reflection and polarization characteristics of selected natural and artificial surfaces. T. I. S. Rept. R65SD4, General Electric Co., Philadelphia, 137 pp.

Earing, D. G., and J. A. Smith, 1966: Data compilation: Target signatures analysis center. Inst. Sci. Tech., University of Michigan.

Gates, D. M., and W. Tantraporn, 1952: The reflectivity of deciduous trees and herbaceous plants in the infrared to 25 μ. *Science*, **115**, 613–616.

——, H. G. Keegan, J. C. Schleter and V. R. Weidner, 1965: Spectral properties of plants. *Appl. Opt.*, **4**, 11–20.

Hapke, B. W., 1963: A theoretical photometric function for the lunar surface. *J. Geophys. Res.*, **68**, 4571–4586.

——, and H. Van Horn, 1963: Photometric studies of complex surfaces, with applications to the moon. *J. Geophys. Res.*, **68**, 4545–4570.

Kondratyev, K. Ya., 1969: *Radiation in the Atmosphere.* New York, Academic Press, 431–440 pp.

Krinov, E. L., 1947: Spectral reflection properties of natural surfaces. Tech. Trans. TT-439, Natl. Res. Council of Canada, Ottawa, 1953, 268 pp.

Mullamaa, Yu. A. R., 1964: The reflection of direct radiation from an ocean surface. *Izv. Atmos. Oceanic Phys.*, **8**, 750–757.

Oetking, P., 1966: Photometric studies of diffusely reflecting surfaces with applications to the brightness of the moon. *J. Geophys. Res.*, **71**, 2505–2513.

Orlova, N. S., 1952: Radial diagrams of scattering for several materials. *Tr. Astron. Observ., Leningrad State Univ.*, **16**, 166–193.

Ross, Tu. K., and T. Nil'son, 1963: Theory of the radiation regime of a plant cover. *Esti NSV Tead. Akad. Joim. Fuus. Astron. Inst.*, No. 4, 42–64.

——, and ——, 1968: The radiation regime of plants with horizontal leaves. *Eesti NSV Tead. Akad. Joim. Fuus. Astron. Inst.* No. 9, 5–34.

Salisbury, J. W., and P. E. Glaser, 1964: Studies of the characteristics of probable lunar surface materials. AFCRL Rept. 64–970, Spec. Rept. 20, Bedford, Mass., 309 pp.

Shifrin, K. S., 1953: On the theory of albedo. *Tr. Gl. Geofiz. Observ.*, **39**, 101.